GSA Data Repository Item 2017269
Chevalier, M.-L., Leloup, P.H., Replumaz, A., Pan, J., Métois, M., and Li, H., 2017, Temporally constant slip-rate along the Ganzi fault, NW Xianshuihe fault system, eastern Tibet: GSA Bulletin, doi:10.1130/B31691.1.

DATA REPOSITORY

Figure S1. Field photos of the Ganzi fault. (A) Kasa Lake pull-apart at the NW tip of the Xianshuihe fault, where the Zhuwo fault merges with the Xianshuihe fault (location in Fig. 1C). (B) Fault push-ups in the Ganzi basin. (C) Ganzi fault trace just NW of the Ganzi basin. (D) Pull-apart just NW of the MGT site. Photo locations in Figure 1C. (E) Google Earth image of the area just NW of Ganzi, where push-ups and pull-aparts are aligned along the fault.

Figure S2. Boulders collected for ^{10}Be surface-exposure dating at the ZDG moraine site, with their approximate sizes.

Figure S3. Summary of depth profile data at the MGT site, used in Hidy et al. (2010)'s program. “1 s AMS Error” refers to one sigma error measured by the Accelerator Mass Spectrometer while “1 s Total Error” refers to one sigma total error which includes the AMS error added in quadrature with an estimated 2% 1-sigma error in sample preparation and analysis. Screen shot of the parameters entered into Hidy et al. (2010)'s program for the MGT depth profile samples. We varied the Monte Carlo parameters using 2 sigma confidence level or varying the chi-squared value. Concentrations of ^{10}Be as function of depth below surface.

Figure S4. Boulders collected for ^{10}Be surface-exposure dating at the GZ moraine site, with their approximate sizes.

Figure S5. Left : GPS profiles across de Ganzi fault, using data from Liang et al. (2013) (in red) and Zhao et al. (2015) (in blue) along profile AB in white on the maps to the right. Negative jumps in along-fault velocities stand for left-lateral motion, while positive jumps in across-fault velocities stand for extension. Different slip-rate estimates across the Ganzi fault are indicated in blue or red depending on the velocity field considered. Significant values (i.e. larger than their uncertainty) are placed in boxes. Liang et al. (2013)’s data support a left-lateral rate of 3.3±3.6 to 5.4±2.6 mm/yr, while Zhao et al. (2015)’s data support a left-lateral rate of 1.6±0.9 to 4.4±0.9 mm/yr, depending on the stations considered as representative of the Ganzi fault far-field. Extension rate is found to be 2.7±3.5 to -2.4±2.5 mm/yr following Liang et al. (2013) and 0±0.6 to 1.1±0.8 mm/yr following Zhao et al. (2015). Right : velocity field from Liang et al. (2013) and Zhao et al. (2015) relative to stable Eurasia. The Ganzi fault (GF) is indicated with a bold black line while other major structures in the area are depicted with grey lines. Major cities are indicated.

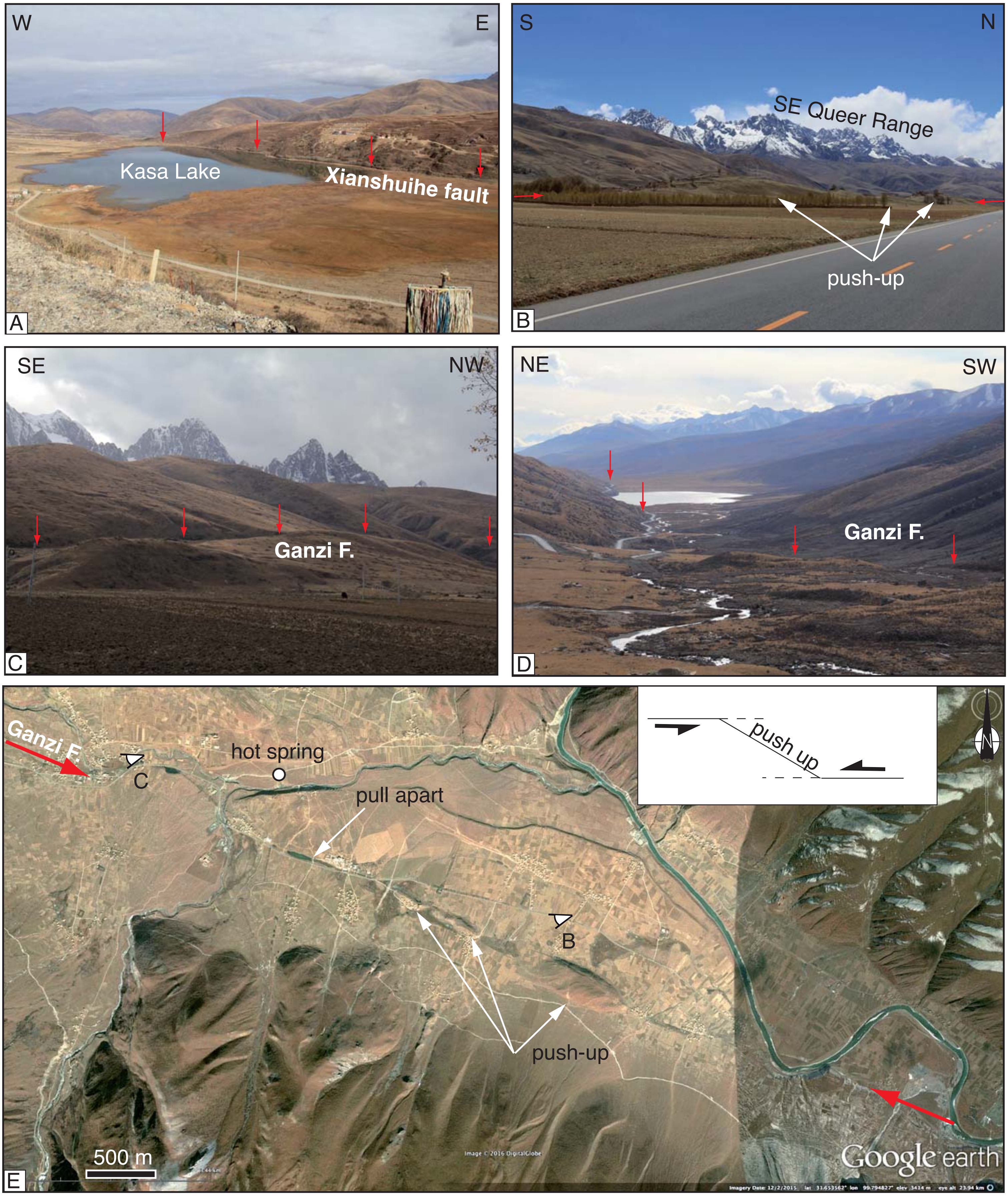

W
E
Kasa Lake
Xianshuihe fault
A
S
N
SE Queer Range
push-up
B
SE
NW
Ganzi F.
C
NE
SW
Ganzi F.
D
Ganzi F.
C
hot spring
pull apart
push up
B
push-up
500 m
Google earth
E


ZDG-1
6x4x3 m
ZDG-1
ZDG-2
3x3x2 m
ZDG-2
ZDG-3
2.5x1.5x0.5 m
ZDG-4
2.5x2x1 m
ZDG-5
6x4x2 m
ZDG-5
ZDG-6
3x1.5x1.5 m
ZDG-7
5x3x2.5 m
ZDG-7
ZDG-8
3x2x0.5 m
ZDG-9
2.5x2.5x2 m
ZDG-10
5x3x2 m
ZDG-10

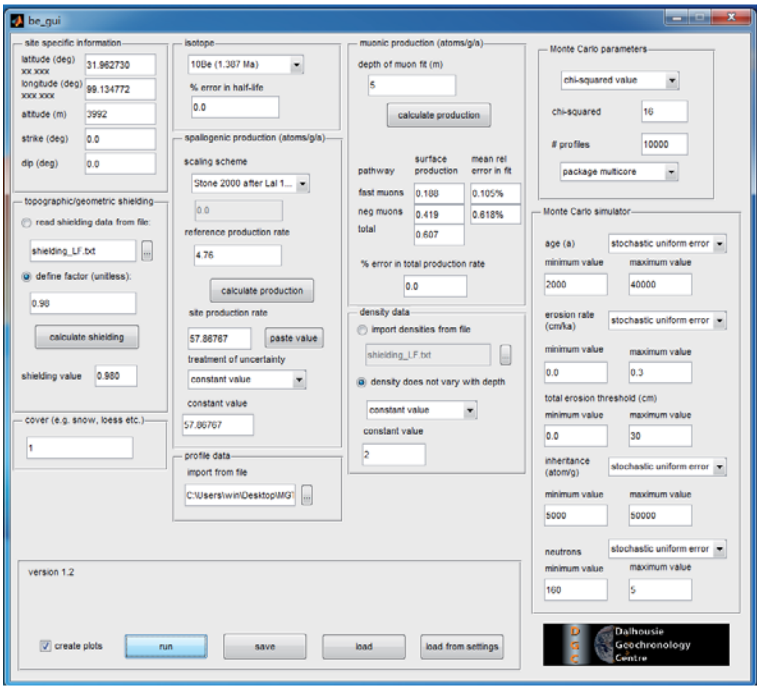

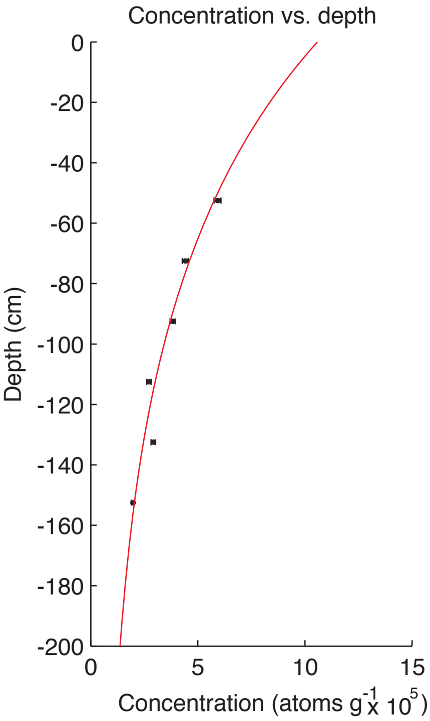

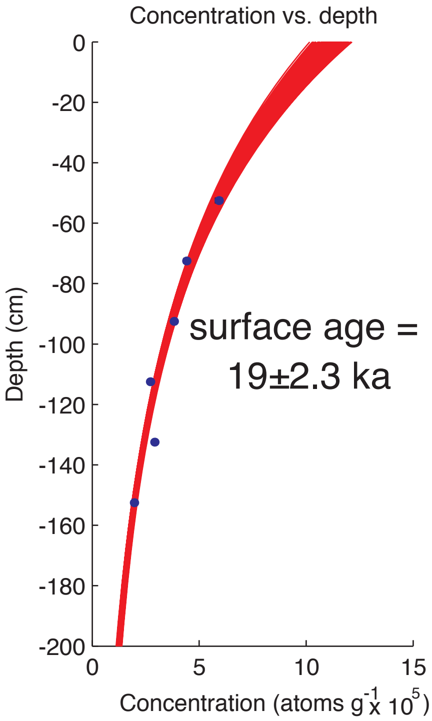

Depth (cm)	Thickness (cm)	10Be conc. (atom/g)	1 s Total Error (%)
50	5	592191	2.71
70	5	441408	3.1
90	5	382448	3.2
110	5	271624	3.69
130	5	291787	3.38
150	5	196664	3.9

	age (ka)	inheritance (10^4 atoms/g)
mean	19.2	3.92
median	19.2	4.07
mode	19.3	4.95
min chi^2	17.7	4.95
maximum	21.3	5.00
minimum	16.5	1.33
Bayesian most probable	19.2	5.00
Bayesian 2-sigma upper	21.0	4.97
Bayesian 2-sigma lower	16.7	1.59


GZ-1
110x80x60 cm
GZ-2
100x60x50 cm
GZ-3
250x150x120 cm
GZ-4
200x120x120 cm
GZ-5
120x70x60 cm
GZ-6
120x70x70 cm
GZ-7
180x140x80 cm
GZ-8
250x70x50 cm
GZ-10B
70x70x40 cm
GZ-11
100x100x50 cm
GZ-12
150x120x60 cm
GZ-13
170x120x60 cm

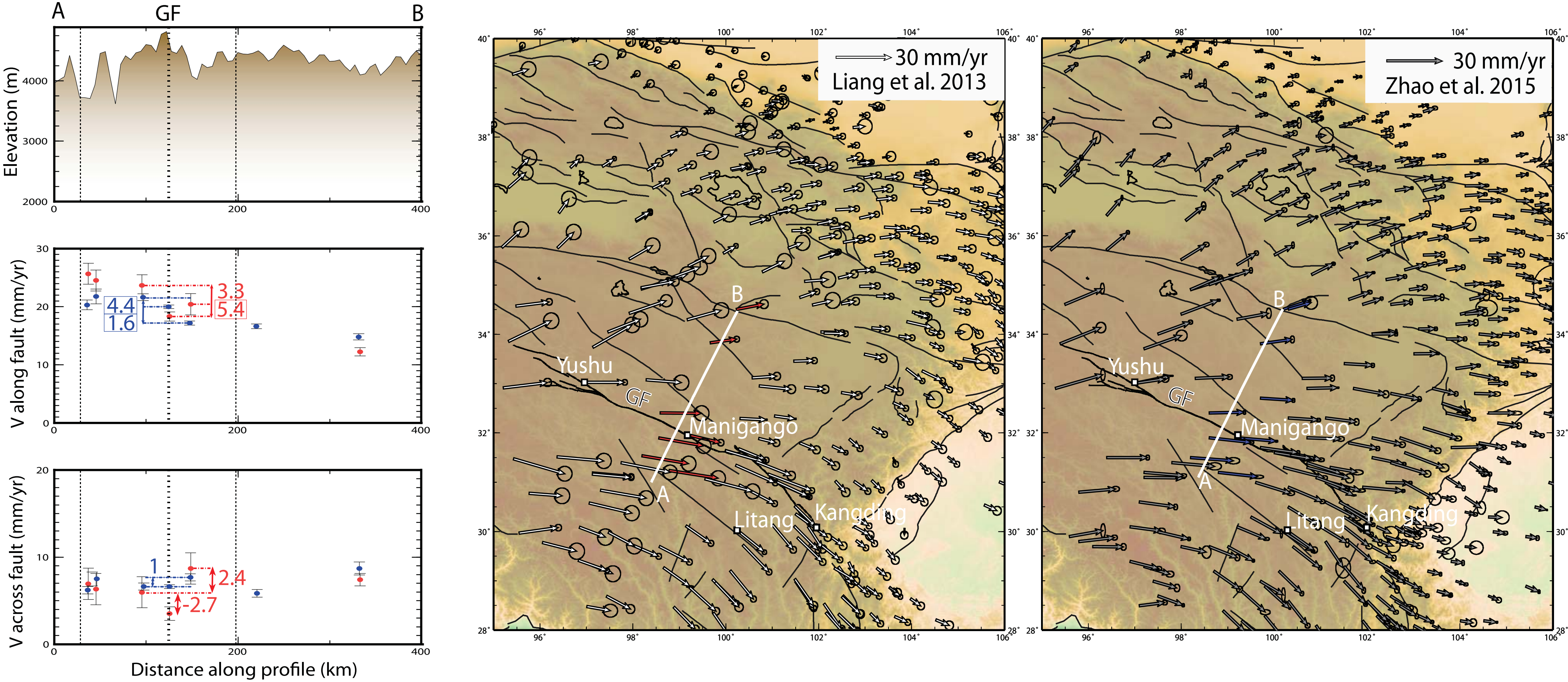

A
GF
B
Elevation (m)
V along fault (mm/yr)
4.4
1.6
3.3
5.4
V across fault (mm/yr)
1
2.4
-2.7
Distance along profile (km)
30 mm/yr
Liang et al. 2013
Zhao et al. 2015
Yushu
GF
Manigango
Litang
Kangding